NANO LETTERS

2008
Vol. 8, No. 8
2305-2309

Comparing Guiding Track Requirements for Myosin- and Kinesin-Powered Molecular Shuttles

Takahiro Nitta,*,† Akihito Tanahashi,† Yu Obara,† Motohisa Hirano,† Maria Razumova,‡ Michael Regnier,‡ and Henry Hess*,§

Department of Mathematical and Design Engineering, Gifu University, Japan, Department of Bioengineering, University of Washington, Seattle, Washington, and Department of Materials Science and Engineering, University of Florida, Gainesville, Florida

Received April 17, 2008; Revised Manuscript Received June 26, 2008

ABSTRACT

The design of nanoscale transport systems utilizing motor proteins as engines has advanced rapidly. Here, actin/myosin- and microtubule/kinesin-based molecular shuttles are compared with respect to their requirements for track designs. To this end, the trajectory persistence length of actin filaments gliding on myosin-coated surfaces has been experimentally determined to be equal to 8.8 ± 2 μm. This measurement complements an earlier determination of the trajectory persistence length of microtubules gliding on kinesin-coated surfaces and enables a comparison of the accessible track designs for kinesin and myosin motor-powered systems. Despite the 200-fold smaller stiffness of actin filaments compared to that of microtubules, the dimensions of myosin tracks for actin filaments have to be quite similar to the dimensions of kinesin tracks for microtubules (radii larger than 200 nm and widths smaller than 0.9 μm compared to 600 nm and 19 μm). The difference in gliding speed is shown to require additional consideration in the design of track modules.

The design of nanoscale transport systems powered by biomolecular motors requires the interfacing of biological elements with a suitably constructed synthetic environment. The design of "tracks" to guide such "molecular shuttles" consisting of cytoskeletal filaments gliding on ATP-consuming motor proteins is a challenging aspect of the development process. Currently, two classes of molecular shuttles are investigated, microtubule/kinesin- and actin/myosin-based molecular shuttles. Two significant differences are the 200-fold larger stiffness of microtubules (MTs) compared to that of actin filaments (AFs)[1] and the 5-fold lower gliding velocities of microtubule/kinesin systems[2] compared to those of the actin/myosin systems.[3] It has been repeatedly pointed out[4–6] that the stiffness of the employed cytoskeletal filament has a strong influence on the track design; stiff microtubules are unable to follow sharp turns, while flexible actin filaments turn unless confined in narrow tracks. The flexible filament and fast gliding speed of actin/myosin molecular shuttle systems have been considered to be major advantages over microtubule/kinesin systems, which enable the design of smaller and faster devices.

Here, these insights are subjected to scrutiny in order to answer the following questions: What is the requirement for track designs for microtubule/kinesin- and actin/myosin-based molecular shuttles? What turn is too sharp, and what track is too wide? Do these parameters reflect the 200-fold higher stiffness of a microtubule compared to that of an actin filament? Does the difference in their gliding speed influence the track designs?

The turning radius is limited by either the amount of force supplied by the motors to force a filament into a turn,[7] the ability of the motors to maintain attachment to the filament despite the elastic restoring forces,[6] or the breaking of the filament due to rupture of the longitudinal bonds between filament subunits.[8] Insufficient forward forces get the filament stuck at a sharp turn; loss of attachment to motors leads to disengagement of the filament from the track; and breaking reduces the forward force by reducing the number of motors bound to a shorter filament and increases the likelihood of disengagement from the surface.[9]

The force-limited turning radius can be estimated by comparing the force generated by the motors along the filament with the derivative of the bending energy of the filament along the contour length, or $r^2 = EI/2F$, with r as the radius, EI the flexural rigidity, and F the collective force of motors.[4] This radius is smaller than the radius observed for spiraling filaments since force generated by motors along

* To whom correspondence should be addressed. E-mail: nittat@gifu-u.ac.jp (T.N.); hhess@mse.ufl.edu (H.H.).
† Gifu University.
‡ University of Washington.
§ University of Florida.

10.1021/nl8010885 CCC: $40.75
Published on Web 07/18/2008

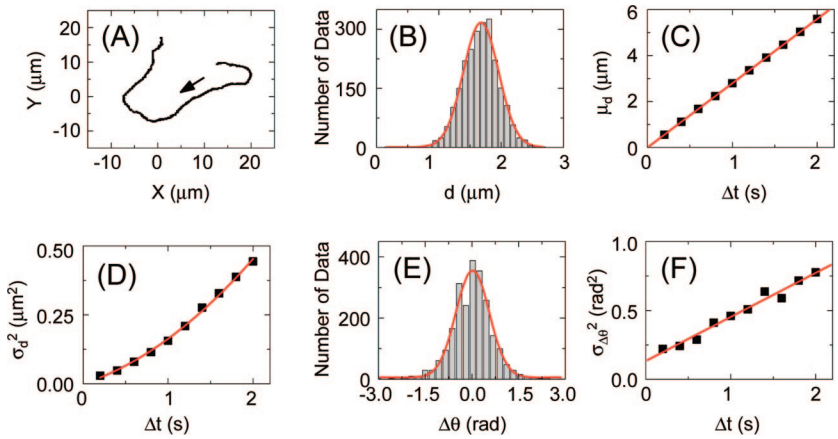

Figure 1. Measurement of trajectory parameters of actin filaments gliding over myosin-coated surfaces. (A) A representative trajectory of an actin filament gliding over a myosin-coated surface. (B) Distribution of distances (d) traveled by actin filaments during 0.6 s and its Gaussian fit. (C) Center μ of the Gaussian fit of the distributions of d (μ_d) as a function of Δt and its linear fit. (D) Variance σ^2 of the Gaussian fit of the d distributions (σ_d^2) as a function of Δt and its fit with a parabolic function (see text). (E) Distribution of directional changes ($\Delta\theta$) of actin filaments during 0.6 s and its Gaussian fit. (F) Variance σ^2 of the Gaussian fit of the $\Delta\theta$ distributions ($\sigma_{\Delta\theta}^2$) as a function of Δt and its linear fit.

the filament is transmitted to the tip and contributes to the bending of the tip.[7] Using an estimate of motor force per unit length of 100 pN/μm for microtubules and 2 pN/μm for actin filaments, which reflects the differences in duty cycles and motor forces between kinesin and myosin,[9] and an estimate of EI of 21 pNμm^2 for microtubules and 0.073 pNμm^2 for actin filaments,[1] the force-limited turning radius is 200 and 80 nm for 3 μm long microtubules and actin filaments, respectively. Sundberg et al. pointed out that the motor−filament bond has to be of sufficient strength in the absence of a physical barrier, which provides the force to bend the filaments.[6] This applies to track designs relying solely on the patterned immobilization of motors, a strategy effective only for the flexible actin filaments.[4] Sundberg et al. calculated a minimum turning radius of 200 nm for actin filaments gliding on myosin.

The breakage-limited turning radius has been determined for actin filaments in detailed experiments to be 200 nm.[8] In vivo, microtubules have been observed to break at a radius of 600 nm,[10] as one would predict from models of the longitudinal tubulin−tubulin bonds[11] and simple mechanics. The turning radius is thus limited to no less than 200 nm for actin filaments and 600 nm for microtubules since enough force can be generated to break the filament independent of the specific estimates of collective motor force or flexural rigidity.[12–14]

On the other hand, the track motif has to be sufficiently small to properly guide the filaments. For example, a straight channel width has to be small enough to prevent the gliding filament from performing a U-turn.[3,4,15] More precisely, the track width has to be smaller than the trajectory persistence length L_p defined by:

$$\langle \cos[\Delta\theta(\Delta t)] \rangle = \exp\left(-\frac{v_{avg}\Delta t}{2L_p}\right) \quad (1)$$

where $\Delta\theta(\Delta t)$ is the directional change of the AF or MT during time interval Δt and v_{avg} is the time-averaged velocity.

The trajectory persistence length L_p is therefore the critical parameter. For microtubules gliding on kinesin-coated surfaces, it has been previously determined that L_p is equal to 111 μm (92−132 μm) in the absence of defect motors and 35 μm (28−44 μm) at typical defect densities,[16] values which are supported by other observations.[17–19] However, this information has not been available for actin filaments.

Here, trajectories of 28 actin filaments gliding on myosin-coated surfaces were analyzed to obtain this information (Figure 1).

The trajectory analysis yielded two previously known parameters,[20] the average velocity, v_{avg}, and the motional diffusion coefficient, $D_{v\text{-}flu}$, as well as two previously unknown parameters, the trajectory persistence length, L_p, and the variance of average filament velocities, $\langle(\Delta v_{avg})^2\rangle$.

Time-Averaged Velocity (v_{avg}): For every trajectory, the distances traveled along its trajectory during a given time step Δt were calculated. Then, histograms of the traveled distances were created for $\Delta t = 0.2$ up to 2.0 s. Figure 1B shows the histogram of the traveled distances during 0.6 s. Since the traveled distances are considered to be the sum of smaller traveled distances which are statistically identical, the central limit theorem can be applied. Therefore, the histograms were fitted with a Gaussian distribution function

$$y = A + B \cdot \exp\left(-\frac{(x-\mu)^2}{2\sigma^2}\right) \quad (2)$$

Figure 1C shows the Δt dependence of μ_d, which is the average traveled distance during Δt, that is, $\mu_d = v_{avg} \cdot \Delta t$. From its linear fit, the time-averaged velocity was calculated to be 2.8 μm/s.

Motional Diffusion Coefficient ($D_{v\text{-}flu}$) and Variance of Average Filament Velocities, $\langle(\Delta v_{avg})^2\rangle$: Figure 1D shows the fit parameter σ^2 in eq 2 as a function of the size of the time step Δt. This variance (σ_d^2) is due to the stochastic nature of myosin motor action, and the heterogeneity of the time-averaged velocity among AFs and can be expressed by

$$\sigma_d^2 = 2D_{v\text{-}flu}\Delta t + \langle(\Delta v_{avg})^2\rangle(\Delta t)^2 \quad (3)$$

From a fit of the above formula to Figure 1D, the motional diffusion coefficient $D_{v\text{-}flu}$ and the variance of the time-averaged velocity among AFs $\langle(\Delta v_{avg})^2\rangle$ were determined to be 5.0×10^{-2} μm^2/s and 6.3×10^{-2} μm^2/s^2, respectively.

Persistence Length of Trajectory (L_p): Expanding the expression in eq 1 for small $\Delta\theta$ and $v_{avg}\Delta t/2L_p$, we obtain

$$\langle(\Delta\theta(\Delta t))^2\rangle = \frac{v_{avg}\Delta t}{L_p} \quad (4)$$

The $\Delta\theta(\Delta t)$ was calculated from all 28 trajectories for $\Delta t = 0.2-2.0$ s. In this range, the estimated error introduced by the expansion of the left-hand side of the eq 1 is at most around 6%. Figure 1E shows the distribution of $\Delta\theta$ of $\Delta t = 0.6$ s. The distribution of $\Delta\theta$ is well fitted with a Gaussian distribution function as defined by eq 2. The dependence of the variance $\sigma_{\Delta\theta}^2$ on the size of the time step Δt is linear (Figure 1F), showing that the higher-order terms of the expansion are negligible. From the slope of the fitted regression line and $v_{avg} = 2.8$ μm/s, L_p was determined to be 8.8 μm (± 2 μm, see below).

The agreement between our measurement and previously reported values for v_{avg} and $D_{v\text{-}flu}$ validates our experiments and analysis. Our value of $v_{avg} = 2.8$ μm/s reproduced our previous results.[21] The obtained value of $D_{v\text{-}flu} = 5.0 \times 10^{-2}$ μm^2/s is comparable with those reported by Noda et al. of 3.7×10^{-2} and 1.5×10^{-2} μm^2/s for AFs gliding along native thick filaments from *M. galloprovincialis* and *S. virgatus*, respectively.[20]

To validate our analysis procedure further,[22] a computer simulation of AF gliding on a myosin-coated planar surface was carried out with $v_{avg} = 2.8$ μm/s, $D_{v\text{-}flu} = 5.0 \times 10^{-2}$ μm^2/s, $L_p = 8.8$ μm, and a time step of $\Delta t = 0.01$ s for a simulated duration of 500 s, which results in a trajectory length comparable to the total trajectory length of all 28 trajectories analyzed. The simulated trajectory was analyzed in the same manner as the experiment, and the parameters were retrieved to be $v_{avg} = 2.8$ μm/s (SD = 0.02 μm/s), $D_{v\text{-}flu} = 5.1 \pm 0.5 \times 10^{-2}$ μm^2/s, and $L_p = 9.3 \pm 1.7$ μm (mean $\pm$ SD; $N = 10$). In addition to validating the analysis method, this provides an estimate of the error of the above-determined trajectory parameters v_{avg}, L_p, and $D_{v\text{-}flu}$.

The actin filament trajectory persistence length of 8.8 μm is plausible since it is expected that the trajectory persistence length is equal to the persistence length of the actin filament at high motor surface densities[9] and the most recent measurement of the actin persistence length found a value of $\sim$8.75 μm,[14] while previously reported values[1,23,24] fall in the range of 5−17 μm. Taking into account the filament-length-dependent persistence length of microtubules,[13,25] our measurements show that the analysis by Duke et al.[9] correctly predicted that the trajectory persistence length and filament persistence length are equal.

We simulated the gliding of filaments in straight tracks using a previously introduced Monte Carlo method[26] and found (Figure 2) that the average distance traveled in units of persistence length (under the assumption of perfect guidance) between two successive U-turns scales with

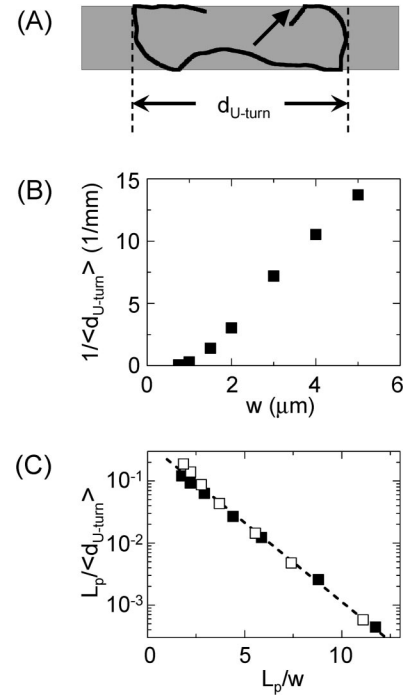

Figure 2. Simulation of actin filament movement through a straight channel. The simulations were carried out with $v_{avg} = 2.8$ μm/s, $D_{v\text{-}flu} = 5.0 \times 10^{-2}$ μm^2/s, and $L_p = 8.8$ μm. (A) A representative actin filament trajectory (black line) making a U-turn in a straight channel of 3 μm width (gray region). The direction of the actin filament movement is indicated by the arrow. The distance between two successive U-turns is denoted by $d_{U\text{-}turn}$, as shown in the figure. (B) Frequency of U-turns (defined as the reciprocal of the average of $d_{U\text{-}turn}$) as a function of the straight channel width (w). Decreasing the channel width w rapidly decreased the U-turn frequency. (C) The scaling relationship between L_p/w and $L_p/\langle d_{U\text{-}turn}\rangle$. Plots of AFs (solid squares) and MTs (open squares) collapsed onto a single line: $L_p/\langle d_{U\text{-}turn}\rangle = 0.4\cdot\exp(-0.6\cdot L_p/w)$. MT simulations were carried out as described elsewhere.[26]

$\exp(-0.6\cdot L_p/w)$, where w is the track width. The determination of the scaling relationship illustrates the value of the Monte Carlo simulation since we were unable to deduce this relationship analytically.

The maximum track width supporting a typical transport distance[6,16,27] of 1 mm for more than 90% of MTs or AFs is thus 19 and 0.9 μm for microtubules ($L_p = 111$ μm) and actin filaments ($L_p = 8.8$ μm), respectively (Figure 2). Here, it is assumed that escape is impossible (e.g., due to improved wall designs[18,28,29]). Furthermore, the impact of defective motors, which can temporarily immobilize the tip of the advancing filament and cause a random redirection,[30] is not taken into account in this discussion.

The design of a concentrator is presented here to demonstrate the insight that the difference in their gliding speed does impact track designs. In our simulations, although most MTs and AFs in a concentrator moved around the circular edge and "jumped over" the junction with the inlet channel (as indicated by the arrows in Figure 3A), a fraction of MTs and AFs made sharp turns around the junction or before and "leak out" (as indicated by the dotted arrow in Figure 3A) with a characteristic time constant (Figure 3B). Although the dimensions of the circular concentrator of Design 1 were

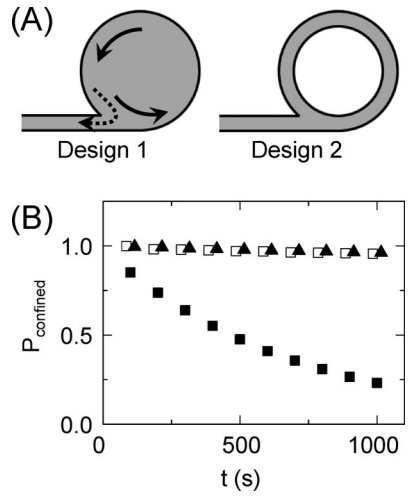

Figure 3. (A) Concentrator designs. Circular concentrator, Design 1: the radius of the circle was set to be $L_p/5$, and the width of the inlet channel was set to be $L_p/20$. Ring concentrator, Design 2: the outer radius of the ring was set to be $L_p/5$, andn the width of the channel was set to be 250 nm. (B) Simulated time evolutions of the fraction of AFs (solid squares) and MTs (open squares) confined in the concentrators of Design 1 and AFs confined in the concentrator of Design 2 (solid triangles). For better visibility, plots of MTs of Design 1 and AFs of Design 2 were slightly shifted horizontally. AF simulations were carried out with $v_{avg} = 2.8$ μm/s, $D_{v\text{-}flu} = 5.0 \times 10^{-2}$ μm^2/s, and $L_p = 8.8$ μm; MT simulations were carried out as described elsewhere.[26] One thousand trajectories were generated for each of five simulations.

scaled with the respective persistence lengths L_p for AFs and MTs, the characteristic "leakage" times showed a 40-fold difference, $6.9 \pm 0.3 \times 10^2$ s and $3.0 \pm 0.4 \times 10^4$ s (mean $\pm$ SD; $N = 5$) for AFs and MTs, respectively. This is consistent with dimensional analysis, which shows that the characteristic time scales with L_p/v_{avg} since the relevant parameters are L_p and v_{avg} only. To confine AFs longer, a better track motif has to be utilized. For example, by utilizing a ring concentrator of Design 2 in Figure 3A, AF confinement is 40-fold improved (the characteristic time constant of $2.7 \pm 0.3 \times 10^4$ s (mean $\pm$ SD; $N = 5$).

In conclusion, the minimum turning radius (0.2 μm for AFs, 0.6 μm for MTs) and the maximum channel width (0.9 μm for AFs, 19 μm for MTs) define boundaries for the design of tracks for molecular shuttles powered by motor proteins. These boundaries may be further constrained by additional considerations, such as the interactions between shuttles.[31] The increase in the maximum channel width from actin filaments to microtubules, however, has a dramatic impact on fabrication. Structures for the control of microtubule guiding can be routinely fabricated by photolithography,[32–35] while control of actin filament transport is best accomplished by structures fabricated by e-beam lithography.[15,36]

Our detailed analysis supports the general statement that flexible filaments and fast motors are desirable. In other words, fast transport in small tracks yields quick results.

While the above discussion facilitates the evaluation of potential devices powered by biomolecular motors, for example, with applications in biocomputation,[37] the key advance here is the determination of the statistical parameters describing the trajectories of actin filaments (L_p, $D_{v\text{-}flu}$, v_{avg}), which enables the design and testing of actin/myosin-based devices in silico using the previously introduced Monte Carlo method.[26]

Hypothetically asking for a filament material which increases the accessible "design space", we are searching for a small modulus combined with high toughness, a combination exemplified by tire rubber (see also refs 38 and 39). It will be interesting to see if future efforts to design synthetic motors and filaments can improve on the properties of biomotors and cytoskeletal biopolymers.

Methods: ***Actin and Myosin Preparation***. Fast skeletal myosin was obtained from the psoas muscle of male New Zealand white rabbits (3−3.5 kg). The rabbits were killed with 50 mg kg^{-1} of sodium pentabarbitol in the marginal ear vein, in accordance with NIH animal care policy and as approved by the University of Washington Animal Care Committee. Skeletal myosin was prepared according to the methods of Margossian and Lowey[40] and stored at −20 °C in a high phosphate solution (0.5 mM KCl, 10 mM $NaHPO_4$, 2 mM $MgCl_2$, 1 mM DTT) mixed with 50% glycerol. Aliquots of the glycerinated myosin stock were digested to heavy meromyosin (HMM) with tosyl lysine chloromethyl ketone (TLCK)-chymotrypsin (Sigma); HMM was stored at 4 °C and used for no more than a week. Daily aliquots of HMM (0.46 mg/ml) were also centrifuged with actin to remove denatured enzyme, as previously described.[41] Rabbit skeletal F-actin was prepared from acetone powder,[42] labeled with rhodamine phalloidin (Molecular Probes, Eugene, OR, U.S.A.), as described by Kron et al.,[43] stored at 4 °C, and used up to 6 weeks.

In Vitro Motility Assay. In vitro motility assay experiments were performed according to the standard protocol[43] using actin buffer (AB) consisting of 25 mM imidazole, 25 mM KCl, 4 mM $MgCl_2$, 1 mM EGTA, and 1 mM DTT at pH 7.4 at 23 °C. Filament motility was collected in AB plus 2 mM ATP, 50 mM ionic strength, pMg = 3, and containing antioxidizing agents (0.018 mg mL^{-1} catalase, 0.1 mg mL^{-1} glucose oxidase, 3 mg mL^{-1} D-glucose, 40 mM DTT) to delay photobleaching of the rhodamine label and inhibit photo-oxidative protein damage. All experiments were performed at 23 °C (range: 22.9−23.1 °C), with the temperature periodically checked by a thermocouple (model BAT-10R, Physitemp, Clifton, NJ, U.S.A.). The flow cell temperature was maintained by circulating water through a copper coil wrapped around the objective.

Filaments were visualized via fluorescence microscopy using a 100× objective and illumination by a 100 W HBO Hg lamp (Zeiss). More than 80% of AFs were moving. The length of the shortest AF which glided smoothly was 0.4−1 μm (2−5 pixel). AF movements were recorded using a SIT camera on video tapes. The movies were digitalized using Adobe Premiere software. The trajectories were obtained using Metamorph software by recording the position of the leading ends at a frame rate of 5 frames/s. Trajectories whose ratio was between the standard deviation and the mean of the traveled distance during 0.2 s was less than 0.35 were

accepted. Twenty-eight AF trajectories were collected. The lengths of the tracked actin filaments varied from 2 to 18 μm. As previously reported,[44,45] there was no systematic difference in velocities within this range of the filament length.

Simulation Method. The simulations were performed according to the method described in detail elsewhere.[26] Briefly, AF or MT movement in a microfabricated pattern was described as a two-dimensional random walk having a persistence length and being confined in a region. The random walk was generated with an off-lattice Monte Carlo simulation. The step distance (r) and angular change ($\Delta\theta$) during a time step (Δt) were random variables with Gaussian distributions. Their means and variances were given by

$$\bar{r} = v_{\text{avg}}\Delta t$$

$$\overline{(r-\bar{r})^2} = 2D_{\text{v-flu}}\Delta t$$

$$\overline{\Delta\theta} = 0$$

$$\overline{\Delta\theta^2} = \frac{v_{\text{avg}}\Delta t}{L_{\text{p}}}$$

where v_{avg} is the time-averaged velocity, $D_{\text{v-flu}}$ is the motional diffusion coefficient, and L_{p} is the persistence length of the AF or MT trajectory. These values for MT have been experimentally determined.[16] The ones for AF were determined as described in the preceding section of this paper. The time step was set to be an order of magnitude smaller than the time required to traverse the smallest structure studied ($\Delta t = 0.01$ s and 0.1 for AF and MT, respectively). For every time step, it was checked if the AF or MT crossed track boundaries. If the AF or MT did not cross the boundary, the location was employed as the next location. If the AF or MT crossed the boundary, the AF or MT was guided along the boundary, that is, the segment of the AF or MT trajectory outside of the track boundary was folded onto the boundary, and the direction of the AF or MT was set to be tangential with the boundary. It was assumed that no AFs and/or MTs escaped from the track or showed any preference for moving along the track boundary.

Acknowledgment. We thank Charles Luo for protein purification and labeling. T.N. acknowledges the support of the JGC-S scholarship foundation and thanks Prof. Wendy Thomas of the University of Washington for serving as a host of the visiting scholarship of T.N. M.R. acknowledges HL61683. H.H. is supported by NSF Award DMR0645023.

References

(1) Gittes, F.; Mickey, B.; Nettleton, J.; Howard, J. *J. Cell Biol.* **1993**, *120*, 923–934.
(2) Stracke, P.; Bohm, K. J.; Burgold, J.; Schacht, H. J.; Unger, E. *Nanotechnology* **2000**, *11*, 52–56.
(3) Suzuki, H.; Yamada, A.; Oiwa, K.; Nakayama, H.; Mashiko, S. *Biophys. J.* **1997**, *72*, 1997–2001.
(4) Hess, H.; Clemmens, J.; Matzke, C. M.; Bachand, G. D.; Bunker, B. C.; Vogel, V. *Appl. Phys. A* **2002**, *75*, 309–313.
(5) Clemmens, J.; Hess, H.; Lipscomb, R.; Hanein, Y.; Boehringer, K. F.; Matzke, C. M.; Bachand, G. D.; Bunker, B. C.; Vogel, V. *Langmuir* **2003**, *19*, 10967–10974.
(6) Sundberg, M.; Bunk, R.; Albet-Torres, N.; Kvennefors, A.; Persson, F.; Montelius, L.; Nicholls, I. A.; Ghatnekar-Nilsson, S.; Omling, P.; Tagerud, S.; Mansson, A. *Langmuir* **2006**, *22*, 7286–7295.
(7) Bourdieu, L.; Duke, T.; Elowitz, M. B.; Winkelmann, D. A.; Leibler, S.; Libchaber, A. *Phys. Rev. Lett.* **1995**, *75*, 176–179.
(8) Arai, Y.; Yasuda, R.; Akashi, K.; Harada, Y.; Miyata, H.; Kinosita, K.; Itoh, H. *Nature* **1999**, *399*, 446–448.
(9) Duke, T.; Holy, T. E.; Leibler, S. *Phys. Rev. Lett.* **1995**, *74*, 330–333.
(10) Waterman-Storer, C. M.; Salmon, E. D. *J. Cell Biol.* **1997**, *139*, 417–434.
(11) VanBuren, V.; Cassimeris, L.; Odde, D. J. *Biophys. J.* **2005**, *89*, 2911–2926.
(12) Janson, M. E.; Dogterom, M. *Biophys. J.* **2004**, *87*, 2723–2736.
(13) Pampaloni, F.; Lattanzi, G.; Jonas, A.; Surrey, T.; Frey, E.; Florin, E.-L. *Proc. Natl. Acad. Sci. U.S.A.* **2006**, *103*, 10248–10253.
(14) Liu, X.; Pollack, G. H. *Biophys. J.* **2002**, *83*, 2705–2715.
(15) Bunk, R.; Klinth, J.; Montelius, L.; Nicholls, I. A.; Omling, P.; Tagerud, S.; Mansson, A. *Biochem. Biophys. Res. Commun.* **2003**, *301*, 783–788.
(16) Nitta, T.; Hess, H. *Nano Lett.* **2005**, *5*, 1337–1342.
(17) Clemmens, J.; Hess, H.; Howard, J.; Vogel, V. *Langmuir* **2003**, *19*, 1738–1744.
(18) van den Heuvel, M. G. L.; De Graaff, M. P.; Dekker, C. *Science* **2006**, *312*, 910–914.
(19) van den Heuvel, M. G. L.; Bolhuis, S.; Dekker, C. *Nano Lett.* **2007**, *7*, 3138–3144.
(20) Noda, N.; Imafuku, Y.; Yamada, A.; Tawada, K. *Biophysics* **2005**, *1*, 45–53.
(21) Clemmens, E. W.; Entezari, M.; Martyn, D. A.; Regnier, M. *J. Physiol. (London)* **2005**, *566*, 737–746.
(22) Imafuku, Y.; Toyoshima, Y. Y.; Tawada, K. *Biophys Chem* **1996**, *59*, 139–153.
(23) Yanagida, T.; Nakase, M.; Nishiyama, K.; Oosawa, F. *Nature* **1984**, *307*, 58–60.
(24) Riveline, D.; Wiggins, C. H.; Goldstein, R. E.; Ott, A. *Phys. Rev. E* **1997**, *56*, R1330–R1333.
(25) Kis, A.; Kasas, S.; Babic, B.; Kulik, A. J.; Benoit, W.; Briggs, G. A. D.; Schonenberger, C.; Catsicas, S.; Forro, L. *Phys. Rev. Lett.* **2002**, *89*, 248101.
(26) Nitta, T.; Tanahashi, A.; Hirano, M.; Hess, H. *Lab on a Chip* **2006**, *6*, 881–885.
(27) Cheng, L. J.; Kao, M. T.; Meyhofer, E.; Guo, L. J. *Small* **2005**, *1*, 409–414.
(28) Hess, H.; Matzke, C. M.; Doot, R. K.; Clemmens, J.; Bachand, G. D.; Bunker, B. C.; Vogel, V. *Nano Lett.* **2003**, *3*, 1651–1655.
(29) Huang, Y. M.; Uppalapati, M.; Hancock, W. O.; Jackson, T. N. *IEEE Trans. Adv. Packag.* **2005**, *28*, 564–570.
(30) Weiss, D. G.; Langford, G. M.; Seitz-Tutter, D.; Maile, W. *Acta Histochem. Suppl.* **1991**, *41*, 81–105.
(31) Boal, A. K.; Bachand, G. D.; Rivera, S. B.; Bunker, B. C. *Nanotechnology* **2006**, *17*, 349–354.
(32) Hiratsuka, Y.; Tada, T.; Oiwa, K.; Kanayama, T.; Uyeda, T. Q. *Biophys. J.* **2001**, *81*, 1555–1561.
(33) Clemmens, J.; Hess, H.; Doot, R.; Matzke, C. M.; Bachand, G. D.; Vogel, V. *Lab on a Chip* **2004**, *4*, 83–86.
(34) Huang, Y. M.; Uppalapati, M.; Hancock, W. O.; Jackson, T. N. *Biomed. Microdevices* **2007**, *9*, 175–184.
(35) van den Heuvel, M. G.; Butcher, C. T.; Smeets, R. M.; Diez, S.; Dekker, C. *Nano Lett.* **2005**, *5*, 1117–1122.
(36) Nicolau, D. V.; Suzuki, H.; Mashiko, S.; Taguchi, T.; Yoshikawa, S. *Biophys. J.* **1999**, *77*, 1126–1134.
(37) Nicolau, D. V.; Nicolau, D. V.; Solana, G.; Hanson, K. L.; Filipponi, L.; Wang, L. S.; Lee, A. P. *Microelectron. Eng.* **2006**, *83*, 1582–1588.
(38) Norton, R. L. *Machine Design: An Integrated Approach*; Prentice Hall: Upper Saddle River, NJ, 2000.
(39) Ashby, M. *Materials Selection in Mechanical Design*, 3rd ed.; Butterworth-Heinemann: Burlington, MA, 2005; p 619.
(40) Margossian, S. S.; Lowey, S. *Methods Enzymol.* **1982**, *85*, 55–71.
(41) Clemmens, E. W.; Regnier, M. *J. Muscle Res. Cell Motil.* **2004**, *25*, 515–525.
(42) Pardee, J. D.; Spudich, J. A. *Methods Enzymol.* **1982**, *85*, 164–181.
(43) Kron, S. J.; Toyoshima, Y. Y.; Uyeda, T. Q. P.; Spudich, J. A. *Methods Enzymol.* **1991**, *196*, 399–416.
(44) Uyeda, T. Q. P.; Kron, S. J.; Spudich, J. A. *J. Mol. Biol.* **1990**, *214*, 699–710.
(45) Toyoshima, Y. Y.; Kron, S. J.; Spudich, J. A. *Proc. Natl. Acad. Sci. U.S.A.* **1990**, *87*, 7130–7134.

NL8010885